JAST, Vol. 10, No. 1, pp. 57- 68

JAST
Journal of Aerospace Science and Technology

Nonlinear Dynamic Modeling and Hysteresis Analysis of Aerospace Hydro-dynamical Control Valves

A. Jafargholi[1] and H. Karimi Mazra-e Shahi[2]

1 and 2. Department of Aerospace Propulsion, Faculty of Aerospace Engineering KNT University

Postal Code: ???, Tehran, IRAN

ajafargholi@mail.kntu.ac.ir

A new procedure for deriving nonlinear mathematical modeling for a specific class of aerospace hydro-mechanical control valves is presented. The effects of friction on the dynamic behavior of these types of valves along with the experimental verifications are also given. The modeling approach is based on the combination of the following three tasks: decomposition of the valve into simple specific subsystems; derivation of the governing equations of each subsystem; and determination of the unknown parameters and coefficients using dynamic and static tests. Dynamic analysis shows that the presence of friction causes the hysteresis phenomenon in these valves and friction force increment causes an increase in the tracking error. On the other hand, excessive reduction of the friction force causes an instable performance. Therefore, a trade-off between the amount of tracking error and stability margins must be considered.

Keywords: Mathematical modeling, Hydro-mechanical valve, Friction, Hysteresis, Dynamic test**.**

NOMENCLAUTURE

A	An orifice cross section area
A_{eff}	Effective cross section area of the control element piston
A_{fb}	Feedback pipe cross section area
$A_{\max}$	Maximum cross section area of the control element
A_{pis}	Control element piston cross section area
A_u	Control element variable cross section area; (depends on the element position)
A_{sh}	Control element pipe cross section area
A_{th}	Cross section area of the fluid passage from the surroundings of the control element
A_{th}^*	Nominal value of A_{th}
a	Speed of sound inside the liquid which passes through the thrust regulator
a_{ij}	Constant coefficient that depends on the control element profile
C_{Br}	Capacity coefficient; $C_{Br}=\frac{V}{a^2}$
C_d	Discharge coefficient
d_{ij}	Constant coefficients which depend on the control element location
d_u	Variable diameter of element depends on the location of element
$F_{fric.\max}$	Maximum friction force
$F_{a.pis}$	Force due to liquid pressure on the effective area in front of the piston
$F_{b.pis}$	Force due to liquid pressure on the effective area behind the piston
F_{fric}	Friction force
F_{sp2}	Flexible force due to spring displacement
$F_{hyd.reac}$	Hydrodynamic force due to flow reaction force on the surface of the control element
$F_{hyd.st}$	Hydrostatic force due to exit pressure and branch pressure on the surface of the control element
F_Σ	Sum of all forces exerted on the moving part of the control device except the friction force
H_{su}	Position of the control element

1. PhD (Corresponding Author)
2. Associate Professor

$\dot{H}_{su}$	Velocity of control element
$\ddot{H}_{su}$	Acceleration of control element
K_{reac}	Hydrodynamic force coefficient
k_{sp2}	Stiffness of the control element spring
L_{Br}	Hydraulic mass coefficient for thrust regulator from inlet area up to the branch region; $L_{Br}=\frac{l_{Br}}{A_{Br}}$
L_i	Hydraulic mass coefficient of outlet paths of the branch
l_{fb}	Length of the feedback pipe
M	Sum of the moving parts mass in the control element
$\dot{m}$	Mass flow rate through a typical orifice
$\dot{m}_{Dr}$	Discharge mass flow rate
$\dot{m}_{in}$	Inlet mass flow rate of the thrust regulator
$\dot{m}_{In.fb}$	Mass flow rate towards the feedback pipe
$\dot{m}_{Or.pis}$	Mass flow rate through orifice on top of the control element
$\dot{m}_{Out1}$	Mass flow rate towards the thrust regulator main outlet
$\dot{m}_{Out2}$	Mass flow rate towards the sensing part outlet
$\dot{m}_{Out.fb}$	Exit mass flow rate of the feedback pipe
P_{Br}	Pressure at the branch point of the thrust regulator valve
$P_{a.pis}$	Pressure at the cavity behind the control element piston
P_{aft}	Pressure at the exit of a typical orifice
P_{bef}	Pressure at the inlet of a typical orifice
$P_{b.pis}$	Pressure in the cavity behind the control element piston
P_{Out1}	Pressure in the main exit region
$P_{In.fb}$	Pressure at the inlet of feedback pipe
$P_{Out.fb}$	Pressure at the outlet of feedback path
R_{Br}	Equivalent hydraulic resistance from the regulator inlet area up to the branch region
R_i	Equivalent hydraulic resistance
R_{th}	Equivalent variable hydraulic resistance
R^*_{body}	Equivalent hydraulic resistance of regulator body
R^*_{th}	Equivalent hydraulic resistance of regulator main control cross section area at the nominal region
r_{Br}	Coefficient describing the characteristic of
	liquid viscosity
V_{fb}	Variable volume of the feedback pipe filled with liquid
V^*_{fb}	Total volume of the feedback pipe
$\overline{V}_{fb}$	Relative volume of the feedback pipe filled with liquid
x_i	Constant values that determine the control element travel which depends on its profile, and at these points the slope of the profile of the control element changes (see Figure 13)
Z	Waste capacity coefficient
ΔP_{HYS}	Command pressure difference at the increasing and decreasing pressure paths in the hysteresis diagram
ρ	Liquid density
ξ_{fb}	Resistance friction coefficient
ξ_{loc}	Local resistance coefficient

INTRODUCTION

Control valves have numerous applications in a wide variety of industries such as mechanical, electromechanical, electro-hydraulic, mechatronic, and aerospace engineering, to name a few. This research concentrates on the nonlinear modeling and performance analysis of a class of control valves with application in aerospace. The number of published works in the open-literature on this subject is very limited. For simple and precise control, accurate knowledge of valve dynamic behavior is necessary. It should be noted that nonlinearities in a control valve are known as major reasons for system oscillation, and they usually result in low control performance. Therefore, it is necessary to be able to accurately model control valves. This is mainly because one has to make sure of stable operations in all operating regimes [1].

Friction plays an important part in accuracy, sensitivity, and stability of tracking systems [2]. Depending on the type of displacement, there may be various kinds of friction, namely, (1) Sliding, (2) Pivoting, and (3) Rolling. In each of these cases, the friction is a kind of force with waste of energy [3]. Depending on the system structure, friction may be determined from the resistance factors; for example, friction force may be proportional to the square of the moving object velocity. This type of friction force is detected in structures such as one-sided pistons, and cylinders which were filled with fluid [4].

The friction force is a function of the direction of motion. At present, there are no methods for calculation of the amount of this force. Also, the dependence of the type of stiction on the velocity is not clear. However, there are some suggestions for evaluating the friction force (e.g., exponential type relations) [5].

The existing models for friction may be classified into two different categories: (1) static models, and (2) dynamic models. The static models are capable of modeling the Coulomb friction, viscous friction, stiction, and the effects of stribeck [16]. The dynamic model of Dahl [17] with one state variable, the dynamic models of Bilman-Sorine [18]-[20] with one or two state variables, and dynamic model of Lugre [17], [21] with one state variable have also been proposed. The Model of Dahl does not consider stiction, and models of Bilman-Sorine and Lugre, being capable of predicting the stiction, can be considered as extensions to the model of Dahl.

Once the valve nonlinearities are identified, it is also necessary to properly compensate their effects. A pressure regulator valve is modeled by Rami et al. and the experimental results are presented for applications which are not so sensitive [6]. Numerical modeling and experimental results for position control in capillary stop valves are considered in [7]. The modeling and control of an electromagnetic valve is carried out by Eyabi et al. The nonlinear aspects such as stiction and hysteresis are also taken into account and experiments are performed to determine the parameters of the nonlinear model [8]. Gölcü and others utilized neural networks to model an automobile engine valve [9]. A model of control valve for a servo pneumatic positioning system is presented by Ning [10]. Choudhury proposes a data-driven model for the stiction phenomena [11]. Nonlinear modeling of solenoid-operated valves is offered by Khoshzaban Zavarehi [12]. Detection of stiction is studied in [13] and [14], and its compensation is discussed in [15].

In [24] a method is described that can detect and quantify stiction, which may exist in control valves, using routine closed loop test data obtained from the process. To quantify stiction in control valves, different identification techniques like "Using a fitted ellipse" and "Clustering Technique" are proposed.

Development of a mathematical model for valves of a hydraulic system is presented in [25]. In [26] a method has been proposed to model a proportional solenoid valve flow hysteresis based on experimental data.

Although the methods presented in [24], [25] and [26] are simple and easy to implement. The model structures being employed generally have no physical parameters and are only mathematical descriptions.

The model development process in this paper is based on the physical characteristics of the system and the obtained model can be used in the structural and operational optimization of the valve.

The major achievement of this paper is the step-by-step modeling of complex hydro-mechanical control valves in aerospace applications. Moreover, the nonlinear effects such as stiction and hysteresis are analyzed. Experimental results are presented to support the analytical discussions. The primary achievements of this research are: (1) the presentation of a modeling methodology for the use in aerospace control valves, (2) the application of the methodology to a real problem, and (3) the design of an experimental setup for validating the friction coefficient.

MODELING ALGORITHM

The modeling algorithm developed is composed of 10 fundamental steps as described below:

1. Specifying the required input information of the mathematical modeling. For example, specifying the type of expected response. Other related input information include: (1) the structure of the valve, (2) the manufacturing technology of the valve, (3) the operating conditions and conditions of the experiments, and (4) the technical specifications available in the related literature.
2. Defining the required experiments with the goal of completing the data acquisition task. The purpose of this step is to provide the necessary input information with the level of detail which has to be included in the model.
3. Simplifying the structure of the valve; then, decomposing it to simple subsystems. The subsystems are defined so as to perform a specific task. Afterward, developing the block diagram of the system.
4. Developing the mathematical model of the subsystems.
5. Determining the required coefficients of the model.
6. Simulating the subsystems.
7. Should the simulation results of Step 6 be satisfactory, then going to Step 8; otherwise, debugging and modifying the subsystem model, and returning to Step 6.
8. Integrating the subsystem subroutines.
9. Simulating the integrated system, and comparing the results with the experiments.
10. Should the comparison results of the previous step be satisfactory, then ending the process. Otherwise, debugging, correcting the model coefficients, modifying the model appropriately, and returning to Step 9.

It should be noted that if the valve is in the design stages, then, Step 2 would not be executed, and the task of “correction of model coefficients based on experiments” would be replaced by “correction by considering the physical and manufactural limitations”.

MODELING CONSIDERATIONS

Basically, while analyzing the control devices of a liquid propellant engine, the control valve equations can be written in two different ways: (1) in the form of equations of motion for the adjusting element, or (2) in

terms of controlled variables (e.g., pressure or flow). In this work, the second approach has been taken.

Before the governing equations required to describe the operation of any system are derived, it is necessary to identify the primary subsystems which define the major system. The primary hydro-dynamical control subsystems of liquid propellant engines are as follows:

1. A mechanical moving part
2. A part allowing the passage of flow (linking part)
3. A part dividing the incoming flow (Branch)

This is a process classification and it may be considered as the basis of deriving mathematical equations which describe the operation of control valves. There are many differences in the subsystems that compose a control valve (e.g. the external shape and operation parameters). However, the equations describing the operation of the control valve have many factors in common. Therefore, the describing equations could be developed in a general format. Then, the specific equations could be derived by considering the structural and operational characteristics of that valve. In this work, the effects of capacity, inertia, and viscosity of the fluid are also taken into account when deriving and studying the governing equations.

ILLUSTRATIVE EXAMPLE

Here, the thrust regulator valve of a liquid propellant engine has been considered as an example problem [22]. The actual location of this valve within the engine is shown in Figure 1. The thrust regulator output affects the gas generator pressure, and in turn, it affects the power produced by turbine. As a result, the angular speed and heads of the pumps are changed, and the instantaneous pressure of the combustion chamber may be controlled. The modeling assumptions are as follow:

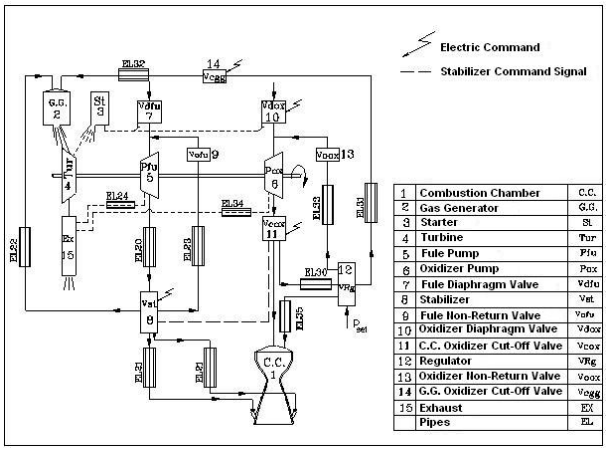

Figure 1. Schematic diagram of a liquid propellant engine [22]

1. The flow in pipes is assumed to be turbulent at steady-state conditions. At transient conditions, the flow may momentarily become laminar; the effects of this are assumed to be negligible.
2. A lumped parameter approach is adopted.
3. Compressibility of the fluid is not assumed.
4. Fluid inertia and fluid viscosity are taken into account.
5. The body of the regulator valve is considered as rigid while the regulator feedback pipe is assumed to be flexible.
6. Dynamics of the regulator feedback pipe are completely taken into account.
7. Filling of the empty spaces within the valve are assumed to be dynamic.

The proposed modeling algorithm is illustrated using the following example.

Step1) As shown in Figure 1, this valve is placed in the oxidizer path. The simplified schematic diagram of the valve is depicted in Figure 2. The primary parts of this valve are: (1) main body, (2) control element, (3) control element piston, (4) sensing element, (5) diaphragm, (6) adjusting spring, (7) auxiliary spring of control element, (8) feedback pipe, (9) filter, (10) adjusting screw, and (11) orifice of the control element piston. This valve has two inputs and three outputs. The inputs are: (1) the flow rate of the incoming liquid and (2) a pressure set point that is mechanically adjusted. The outputs are: (1) the main outgoing liquid flow rate, (2) the auxiliary outgoing liquid flow rate, and (3) the outgoing liquid flow rate towards the path after the feedback pipe.

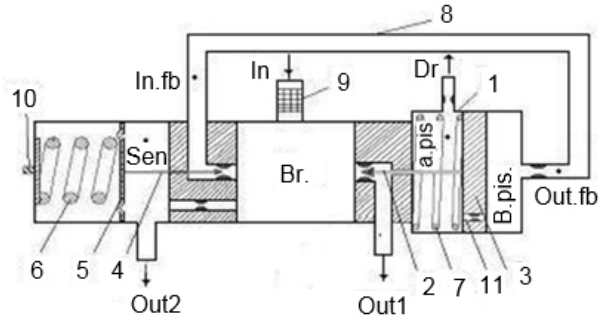

Figure 2. Thrust regulator schematic

After flow passes through the filter 9, the liquid branches out to several parts. Large amount of the incoming liquid travels toward the main output (labeled Out1), and a small amount of the fluid travels towards the auxiliary output (labeled Out2). Finally, another part of the incoming liquid passes through the feedback pipe, and travels towards the back of the control element. Then, throughout the orifice which is located on top of the piston, the liquid travels towards the cavity in front of the control element and the drain gate (labeled Dr).

The operation of the valve is described next. The displacements of the diaphragm and the sensing elements are functions of the difference between the sensing cavity and the set point pressures. Now consider the liquid which passes through the sensing element towards the feedback pipe and to the back of the control element piston. Following the above-mentioned displacements, the pressure drops and the flow rate is changed. Based on the force imposed on the control element, the position of the control element is changed. As a result, it changes the cross section of the passage which leads to change in the pressure drop and the rate of passing fluid flow. This results in recovering the desired output pressure. Therefore, the necessary control is imposed.

It should be noted that the operating region of the thrust regulator is limited, and it depends on the level of command pressure and its variations. If the command level is increased or decreased beyond a certain point, then the regulator would not be able to enforce command signal tracking. In such a condition, the output pressure would remain constant, and the control element gets saturated.

Step 2) The regulator hydraulic test circuit is shown in Figure 3. In this circuit, the input pressure is the input. At a constant set-point, all other flow parameters at different points of the regulator valve are sampled. Also, as it could be seen in the test circuit, the command pressure is received from the region between orifices 1 and 2 at the main exit of the regulator valve. These orifices provide a pressure drop at the exit of the regulator valve. They also ensure that the pressure at the exit of the experimental set-up (P_{out}) is equal to the actual set-up shown in Figure 1. The pressure drop distributions in these two orifices are imposed in such a way that the fluid pressure between these two orifices equals the pressure of the combustion chamber shown in Figure 1. It should be noted that the combustion chamber pressure is the regulator sense pressure. In the experimental set-up, this sensed pressure is "simulated" by the use of these two orifices.

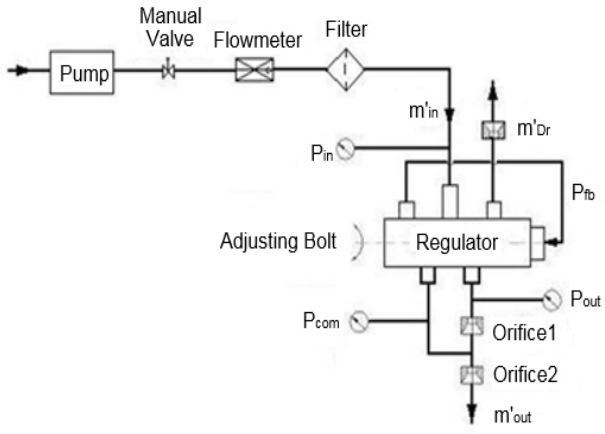

Figure 3. The hydraulic test circuit of regulator

In order to evaluate the friction effects, the hysteresis test circuit is considered as shown in Figure 3. The hydraulic test stand of the regulator is composed of an electric pump, a manual valve downstream of the electric pump, a filter, a flow meter, pressure sensors, pipes, and hydraulic connectors (see Figure 4). In the beginning and before the start of the electric pump, the manual valve is closed. After the start of the electric pump and as soon as the pressure in front of the pump reaches a predetermined value, the manual valve is opened. Then, the fluid passes through the pipe, hydraulic connectors, filter, and the flow meter. Subsequently, the fluid enters the regulator valve. Fluid passes through the regulator, and it goes through orifices 1 and 2. A small amount of fluid ($\dot{m}_{Dr}$) is also discharged through the discharge path (see Figure 4). In this circuit, any changes in the flow pressure drop through the valve is imposed by changes in the command pressure. The certain orifice in the regulator exit path simulates the load in the path after the control device. In order to perform the regulator hysteresis test, the command pressure between orifices 1 and 2 would be disconnected. Then the command pressure would be received from a tank which contains fluid under air pressure. The hysteresis test is performed in the following way. The electric pump is started and fluid passes through the regulator. Then, by adjusting the air pressure above the fluid in the tank, the command pressure is either decreased or increased. Finally, required variables are measured and recorded. The fluid flow variables are measured using magnetic flow meters with an accuracy of 0.2%. The pressure variables are measured using Wetson Bridge pressure sensors with an accuracy of 0.2%.

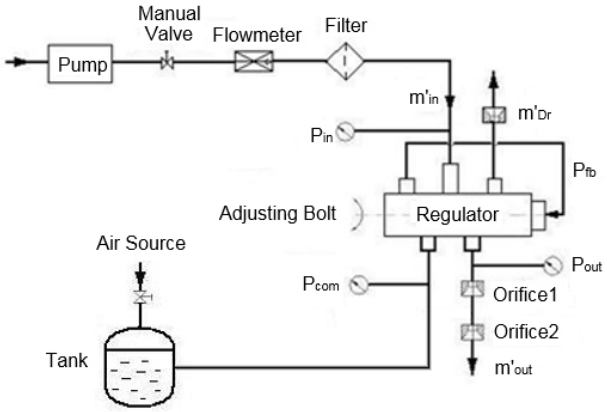

Figure 4. Hysteresis test circuit

It is essential to apply the necessary changes to the command pressure (or the pressure in the "sense" area). This is accomplished by discharging the flow from the regulator branch and the liquid at the output of the "sense" area (Out2) into a water tank. The pressure of the water tank in a stable operating condition of the valve is equal to the nominal

command pressure. The pressure level is controlled by an air feed source that acts on the water column above the water tank. In the hysteresis test process, the pressure at the top of the water tank ullage gradually and continuously increases and decreases. Therefore, the command pressure in the "sense" region of the regulator changes. Now consider the condition where no change is seen at the exit of the thrust regulator valve as the ullage pressure either goes up or down. In this condition, the air pressure is kept constant. After a short pause, the direction of the pressure change gets reversed in the ullage. As a result, the direction of the command pressure also gets reversed.

The adjusting bolt is related to the valve adjustment in the beginning of the work. Depending on the desired exit pressure, the adjusting tasks take place.

Step 3) According to Figure 2 and referring to the primary hydro-dynamical control subsystems which were mentioned before, this control valve is divided into five subsystems:

1. Branch – A part that divides the incoming flow
2. Feedback pipe – A part that allows the passage of flow
3. Control part – A mechanical moving part
4. Sense part – A mechanical moving part
5. Hydraulic connections – Parts that allow the passage of flow

Step 4) The governing equations describing the motion of the thrust regulator valve are derived with respect to the adjusted variable. The obtained force equations are based on Newton's second-law of motion. The equations showing the flow through the orifices as well as the calculation of hydraulic resistances are selected according to [23]. The branch equations are given by [1], and the feedback pipe equations are adopted from [2]. The mathematical models of hydraulic paths are derived on the basis of continuity, norm of the motion and conservation of energy.

The governing equation for each subsystem is given below.

Branch Equations (At point Br based on Figure 2)

$$\frac{dP_{Br}}{dt}=\frac{\dot{m}_{in}-\dot{m}_{Out1}-\dot{m}_{Out2}-\dot{m}_{In.fb}}{C_{Br}}+ r_{Br}\left(\frac{d\dot{m}_{in}}{dt}-\frac{d\dot{m}_{Out1}}{dt}-\frac{d\dot{m}_{Out2}}{dt}-\frac{d\dot{m}_{In.fb}}{dt}\right) \quad (1)$$

Where the mass flow rate variables are given by the following relations:

$$\frac{d\dot{m}_{in}}{dt}=\frac{P_{in}-R_{Br}\dot{m}_{in}\left|\dot{m}_{in}\right|-P_{Br}}{L_{Br}} \quad (2)$$

$$\frac{d\dot{m}_{i}}{dt}=\frac{P_{Br}-R_{i}\dot{m}_{i}\left|\dot{m}_{i}\right|-P_{i}}{L_{i}} \quad (3)$$

In the above relations, the values for R_i are constant for a non-varying cross section area. For branch paths towards the main exit path (Out1) and feedback pipe (In.fb), the values are functions of the flow passage cross section area at each moment. For example, the R_i relation for the branch path towards the main exit path of the thrust regulator valve could be defined as:

$$R_{th}=R^{*}_{bod}+R^{*}_{th}\left(\frac{A^{*}_{th}}{A_{th}}\right) \quad (4)$$

Where, A_{th} is a function of the position of the control element, and is given by the following relation (see Appendix for details).

$$A_{th}=\begin{cases} a_{11}H_{su}{}^{2}+a_{12}H_{su}+a_{13} & 0\le H_{su}\le x_1 \\ a_{21}H_{su}{}^{2}+a_{22}H_{su}+a_{23} & x_1<H_{su}\le x_2 \\ a_{31}H_{su}{}^{2}+a_{32}H_{su}+a_{33} & x_2<H_{su}\le x_3 \end{cases} \quad (5)$$

Feedback Pipe Equations:

$$\frac{l_{fb}}{A_{fb}}\overline{V_{fb}}\frac{d\dot{m}_{Out.fb}}{dt}=P_{In.fb}-P_{Out.fb}\frac{l}{\rho}\left(\xi_{fb}\overline{V_{fb}}+2\xi_{loc}\right)\dot{m}^{2}_{Out.fb} \quad (6)$$

$$\frac{d\overline{V_{fb}}}{dt}=\frac{1}{\rho V^{*}_{fb}}\dot{m}_{In.fb} \quad (7)$$

$$Z\frac{dP_{In.fb}}{dt}=\dot{m}_{In.fb}-\dot{m}_{Out.fb} \quad (8)$$

$$Z=\frac{V_{fb}}{a^{2}} \quad (9)$$

$$V_{fb}=\overline{V_{fb}}.V^{*}_{fb} \quad (10)$$

Control Equations:

$$M\ddot{H}_{su}=F_{b.pis}+F_{hyd.reac}-F_{hyd.st}-F_{a.pis}-F_{sp2}-F_{fric} \quad (11)$$

Where,

$$F_{hyd.st}=P_{Out1}\left(A_{\max}-A_{u}\right)+P_{Br}A_{u} \quad (12)$$

$$F_{sp2}=k_{sp2}H_{su} \quad (13)$$

$$F_{hyd.reac}=K_{reac}.d_{u}^{2}\left(P_{Br}-P_{Out1}\right) \quad (14)$$

$$F_{b.pis}=A_{pis}.P_{b.pis} \quad (15)$$

$$F_{a.pis}=(A_{pis}-A_{sh}).P_{a.pis} \quad (16)$$

In the above relations, the geometric parameters and dimensions depend on the profile of the control element, and they may be calculated using the following relations.

$$A_u = \frac{\pi . d_u^{\,2}}{4} \tag{17}$$

$$d_u = \begin{cases} d_{11} H_{su} + d_{12} & 0 \le H_{su} \le x_1 \\ d_{21} H_{su} + d_{22} & x_1 < H_{su} \le x_2 \\ d_{31} H_{su} + d_{32} & x_2 < H_{su} \le x_3 \end{cases} \tag{18}$$

Detailed information about the development of equation (18) are presented in Appendix. As it is mentioned, the friction term appears in the equation for the resulting force. The equation of the friction force could be expanded as follows.

$$\dot{H}_{su} \neq 0 \quad \text{If} \quad F_{fric} = F_{fric.\max} \frac{\dot{H}_{su}}{\left|\dot{H}_{su}\right|} \tag{19-a}$$

$$\left|F_{\Sigma}\right| \prec F_{fric.\max} \qquad \text{if} \qquad \dot{H}_{su} = 0 \tag{19-b}$$

The physical interpretation of the equations (19-a) and (19-b) could be described as follows:

In the moment when the moving part of the thrust regulator valve passes the point $\dot{H}_{su} = 0$, the friction force may not instantaneously change signs. In the moment that $\dot{H}_{su} = 0$ and F_{Σ} is higher than F_{fric}, motion continues without any delay. But if $-F_{fric.\max} \prec F_{\Sigma} \prec F_{fric.\max}$, the moving part stops. In this condition, the value of F_{fric} is changed in such a manner that $F_{\Sigma} = F_{fric}$ all the time. This means that in each moment, friction equals the other forces and motion will start if $\left|F_{\Sigma}\right| = F_{fric.\max}$.

SENSE EQUATIONS

In the same vein, the equation describing the resultant force as well as the equations for each of the forces produced in the elements of the sensing part could be derived.

CONNECTION EQUATIONS

A typical orifice equation could be written as follows:

$$\dot{m} = C_d A \sqrt{2\rho\left(P_{bef.} - P_{aft.}\right)} \tag{20}$$

The above equation is used to calculate the mass flow rate through the cavity behind the piston toward the cavity in front of that. It is also used to calculate the mass flow rate through the main exit way of the thrust regulator valve.

A typical equation is used to show the relation between the mass flow rates as follows.

$$\dot{m}_{Dr} = \dot{m}_{Or.pis} + \rho A_{pis} \dot{H}_{su} \tag{21}$$

The above equation is used to describe the relation between the leakage mass flow rate and the mass flow rate through the orifice on top of the piston.

Step 5) Generally, the coefficients of the equations are assigned or calculated according to:

- Structural characteristics and manufacturing considerations like spring stiffness and the masses of the moving parts.
- The geometrical and structural dimensions like passageways cross sections areas and effective cross sections of the moving elements.
- The passing flow parameters like discharge coefficients.

It is desired to have a suitable evaluation of the friction force level. It is also desired to properly estimate the effects of friction on the operation of the control device. So, some experimental tests should be performed before the simulation process is commenced. This evaluation takes place by changing the regulator pressure command with respect to the nominal value of the pressure. This continuous pressure change happens once in the way to increasing the command pressure, and once in the way to decreasing that. The increase and decrease of the above-mentioned pressure continues up to a level which the regulator control valve would be saturated. For example, if the command pressure is on increase and the regulator valve becomes saturated, then the increase of the command pressure level will be stopped and the command pressure will start to decrease. The decrease in command pressure is also continued until the valve become saturated again. Then, the decrease in the command pressure stops, and the command pressure starts to increase again until it reaches its nominal value. Due to the existence of the friction force, the regulator exit pressure will change as the command pressure changes in the manner described.

The piston and friction element affect the dynamic behavior of the system as well as the control valve body does. These effects lead to the presence of control pressure difference. This will cause a static error for the regulator control valve. The hysteresis and friction are related as follows [3]:

$$\Delta P_{HYS} = {}^{2F_{fric.\max}}\!\Big/\!_{A_{eff}} \tag{21}$$

While evaluating the regulator errors, the method for calculating hysteresis must consider the operating conditions of the regulator with respect to the structure of the control plant.

Step 6) The simulation of the subsystems under study is accomplished in the SIMULINK environment of MATLAB. This has been done according to the individual simulations for the subsystems of the regulator control valve which are considered in the mathematical model derivation step. To get precise simulation results, the method of integration is set to a

fixed step fourth-order Runge-Kutta with a step size of 1.5 microseconds.

Step 7) By first starting the simulation of the subsystems, the debugging of the SIMULINK code would be easier and it would also allow us to apply any changes to the model easily. At this step, we consider the nominal values for input, output, and internal variables, which would achieve acceptable results. Therefore, after some corrections, the desirable models of the subsystems are obtained.

Step 8) By integrating these subsystems into a unified system, the model is completely developed. The main point in this step is the correct selection of inputs and outputs and their relations with different subsystems.

Step 9) Finally, the developed model will be simulated. The block diagram of the simulated system being studied is shown in Figure 5.

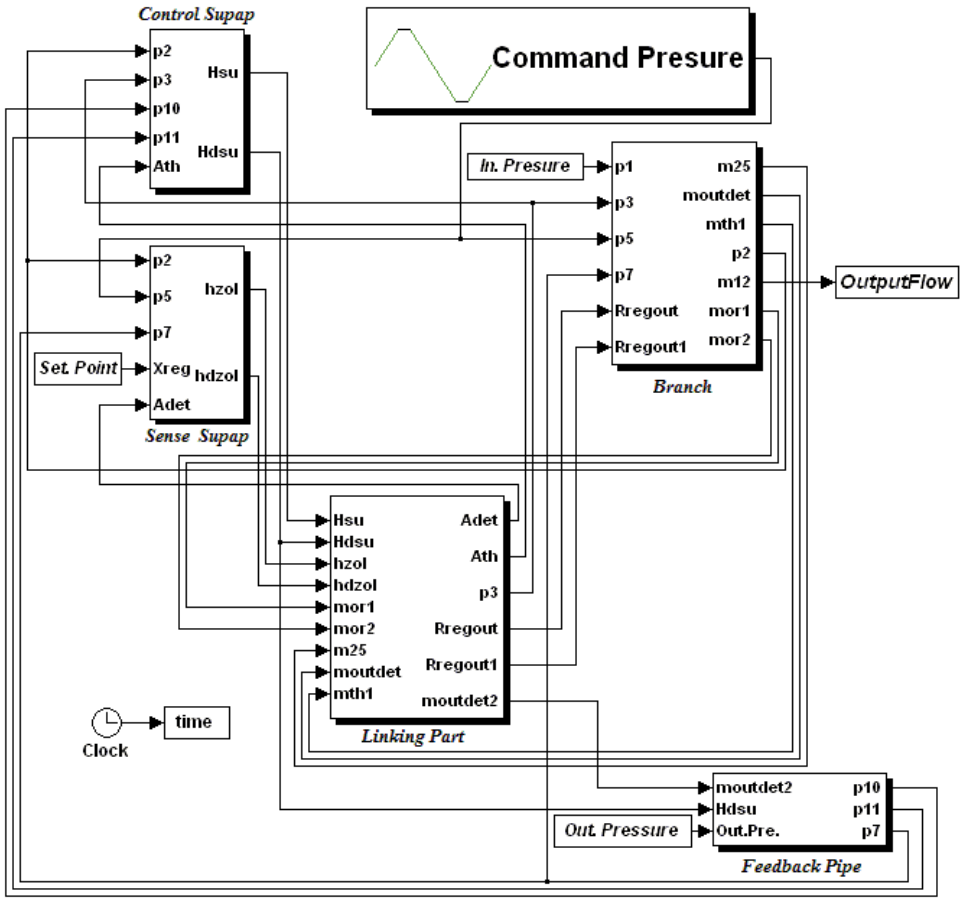

Figure 5. Block diagram of simulating system in SIMULINK

The other important point is applying the correct physical and environmental constraints. As an example, the constraints associated with the sensing and control elements could be mentioned. The method with which the input signals are applied is also important. It should be noted that in the simulation performed, the input pressure, command pressure, and the environment pressure are considered to be the inputs of the simulation. As a result, the entrance flow rate and the exit flow rates are considered to be the outputs of the simulation environment. The mentioned inputs are in fact the outputs from the valve through the orifices, which are results of the simulation of the exit paths at valve outlets.

Step 10) In the mathematical model of the thrust regulator valve it is assumed that the pressure at the entrance of the valve is the input parameter. The pressure changes at the valve entrance are shown in Fig 6. The data is obtained from the recorded changes in the process of hydraulic test, and this data is filtered using a low pass filter with a cut-off frequency of 12.6 rad/sec. The dimensionless simulation and the experimental results are shown in Figs 7 and 8. The percent error between the simulation and experimental data is given in Table 1. The comparison of the simulation and experimental data reveals that both transient and steady-state behaviors are close to each other. The percent error columns are presented in this table. The regulator valve entrance pressure curve is experimentally determined. This curve is then fed into the simulation model. Finally, the variable values obtained from the simulation model are compared to

the corresponding measured values, and the percent errors are calculated from $\left|\frac{Test-Model}{Test}\right|*100$.

Table 1. Transient and steady states error of the simulated model

The Variable	%Maximum Error in Transient State	%Steady State Error
Input flow	5.6%	1.1%
Output pressure	11%	0.5%
Output flow	4.1%	1%
Leakage flow	5.3%	4.3%
Command pressure	11%	0.33%

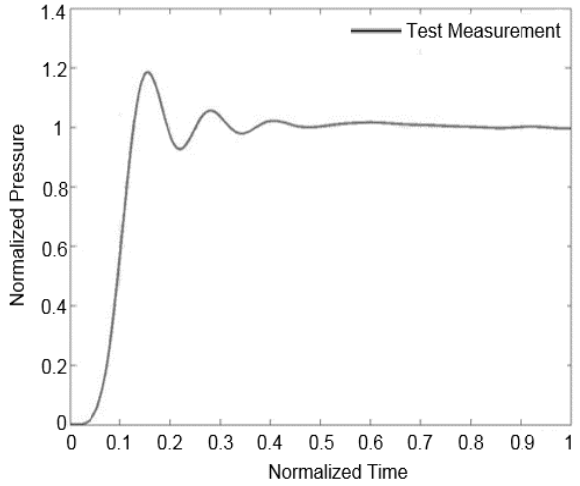

Figure 6. Regulator non-dimension input pressure from test results

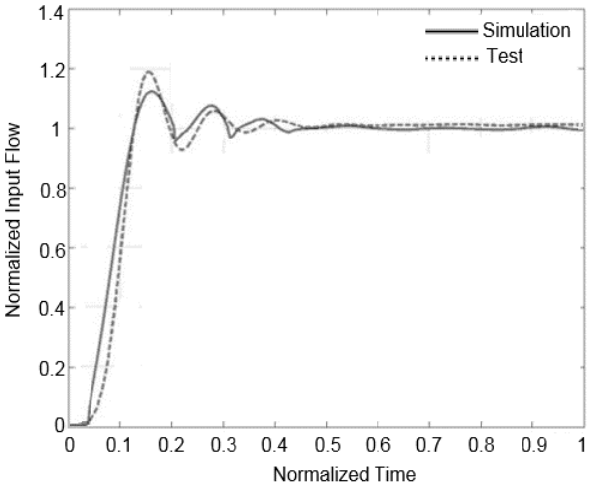

Figure 7. Time responses of simulation and experimental input flow

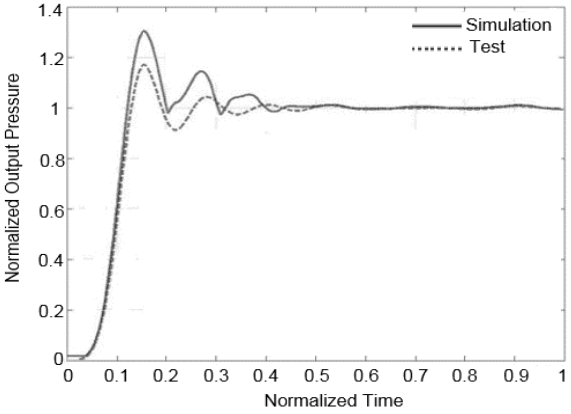

Figure 8. Time responses of simulation and experimental output pressure

In the process of studying the effects of friction on the operation of the regulator, a suitable simulation of the command signal is critical. In other words, the rate of the changes of command signals must be selected by considering the time constants of the valve. So, there would be enough time for the response to the changes of the command signal. It should be noted that the time constant of thrust regulator valve is calculated according to the valve response to a step excitation. The range of the applied changes for command signal in the simulation process should also be selected in correspondence with that of the experiments. Referring to this fact, the command signal which is used in simulations is shown in Fig 9.

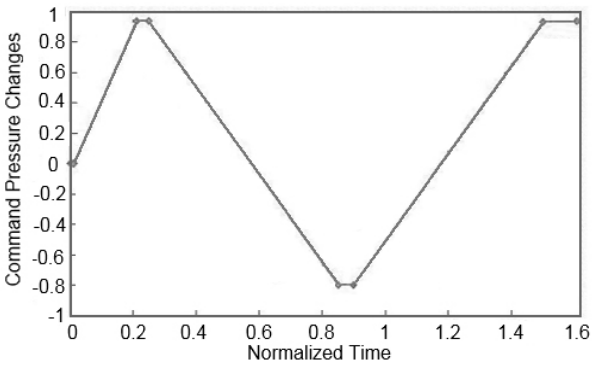

Figure 9. Command signal

In Fig 10, the non-dimensional results for changes in the exit pressure according to the applied changes in the command signal (which are shown in Fig 9) are compared with the simulation and experimental data. The top and bottom points of the curve in this Figure correspond to valve saturation, while the control element has reached the end of its journey. The left and right sides of the curve imply different exit pressures for the same command pressure at the increase and decrease paths. The width of the curve represents the amount of the error in operation process

of the regulator valve (i.e. the wider the curve, the more the operational error). The reasonable accordance of the simulation and experimental results indicates that an acceptable model has been obtained.

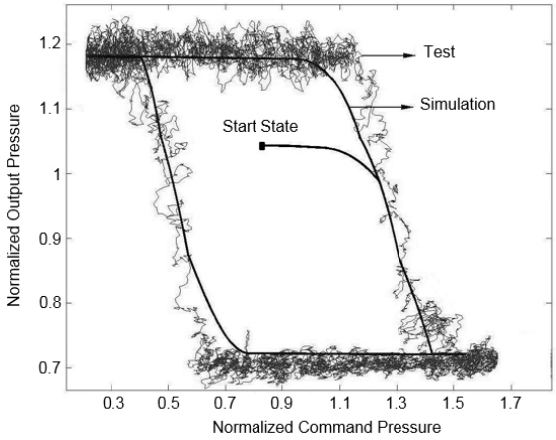

Figure 10. Comparison of simulation and experimental hysteresis curves

Fig 11 shows the hysteresis curves obtained under three different conditions: (1) modeled friction, (2) reduction of the friction force and (3) increase of the friction force because of the value used in the model. As it is shown, while this force is reduced, the differences between the specifications of the control device in the back and forth paths (i.e., when the control device pressure drop is increased and decreased) are reduced. Also, by the increase of friction, these differences are amplified. It is further noted that in this Figure, the effects of changes in friction on the bandwidth of the hysteresis curve may be observed. An increase in friction causes an increase in the hysteresis bandwidth. This causes a decrease in dynamic accuracy of the control valve. Similarly, a decrease in friction causes a decrease in the hysteresis bandwidth and an increase in the dynamic accuracy of the control valve. It should be kept in mind that an excessive decrease in friction may cause an oscillatory behavior of the valve and the liquid engine.

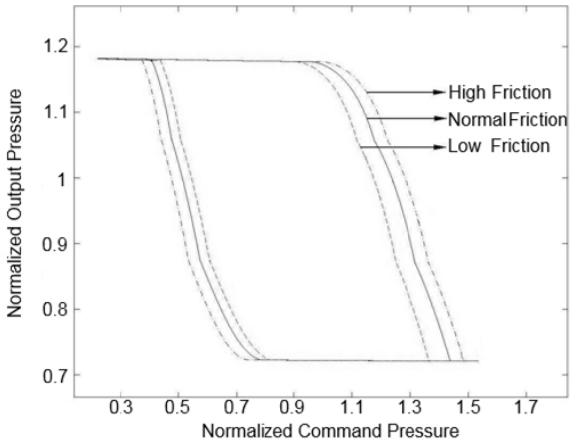

Figure 11. Evaluation of friction changes effects on hysteresis curve

Fig 12 corresponds to the condition that friction force is intensely reduced. Under this condition, oscillations in exit pressure as a function of the sense pressure are observed. This indicates instability of the control device.

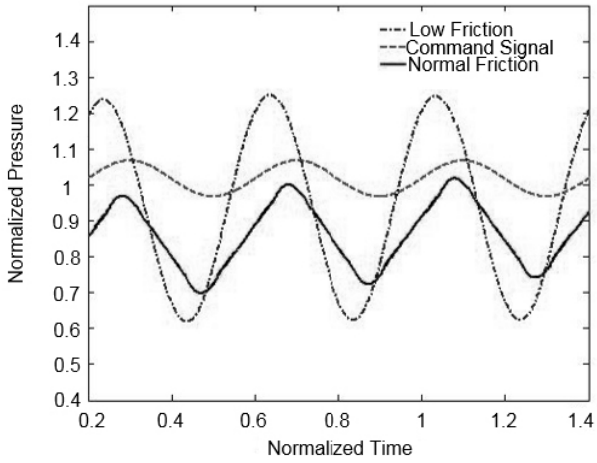

Figure 12. Evaluation of friction changes effects on dynamic response

CONCLUSIONS

In this work, a new procedure for modeling the dynamic behavior of aerospace control valves is presented. The procedure is demonstrated by modeling a thrust regulator valve of a liquid propellant engine. At first, the valve is divided into several subsystems, and the model for each of the subsystem is developed. Finally, the subsystems are connected to form a unit system. The modeling procedure is given in form of an algorithm, and for the evaluation purpose, the modeling results of an example problem are compared with the experimental results. An acceptable accordance between these data is observed. Additionally, the effects of friction on the dynamic behavior of the regulator valve are studied. It is observed that the presence of friction causes the hysteresis phenomenon which is a source of error for the operation of the control device (i.e., the regulator valve).

It has been concluded that as the friction force increases, the tracking error of the regulator valve will increase. From this point of view, it would be desired to decrease the amount of friction force. However, as the friction force decreases, the degree of stability of the valve will also decrease. Therefore, there is a desired trade-off between the reduction of tracking error and the increase in the degree of stability of the regulator valve.

APPENDIX

Details of equations (5) and (18) are given in this Appendix. The cross section area of the fluid passing through the sides of the control actuator is equal to the side area of an incomplete cone as shown in Fig 13.

The *ruff* of the cone (the length Ah), is equal to the perpendicular line which is dropped from the edge of the control hole (point A) to the surface of the control actuator at point h. In order to calculate the cross section of the passing flow, the following steps could be executed.

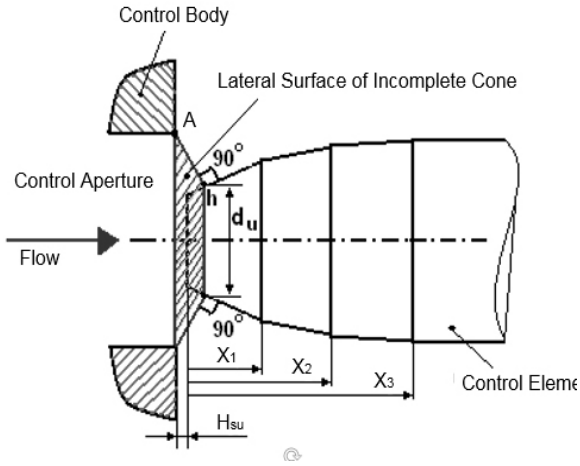

Figure13. Geometry of the control element

1. The x-axis is allowed to coincide with the axis of the control actuator (the dotted line). The baseline is taken to be at the edge of the actuator. Such a coordinate system would be motionless with respect to the control actuator. Therefore, when the actuator is moving, the equations of the points on the surface of the actuator would not change; however, only the coordinate length of point A (x_A) would change.
2. The line equations corresponding to the three slopes on the surface of the actuator are written.
3. The coordinate of point h is determined in the following manner. The equation of the perpendicular line is written, and with each of the line equations of Step 2 above, a system of two equations with two unknowns is solved.
4. The coordinates x_h and y_h in terms of x_A are obtained.
5. Using y_h, d_u is calculate.
6. The length of the perpendicular line Ah in terms of x_A is detrmined. Then, the control cross section A_{th}, which is equal to the incomplete cone side surface area, can be calculated.

REFERENCES

1. Shevyakov A.A., MAI Publication, Theory of automatic control of rocket Engine, 1978, in Russian.
2. Belyaev E.N., Chevanov V.K., Chervakov V.V., MAI Publication, Mathematical model of process, 1999, in Russian.
3. Glikman B.F., Mashinostroyenie Publication, Automatic control of propellant rocket Engine, 1974, in Russian.
4. Prisnyakov V.F., Mashinostroyenie Publication, Dynamic of rocket engine, 1983, in Russian.
5. Dupont P., Hayward V., Armstrong B., and Altpeter F., “Single State Elastoplastic Friction Models,” IEEE Transactions on Automatic Control, Vol. 47, No. 5, May 2002.
6. Rami E. G., Jacques B. J., Bruno D., and François M., "Modeling of a Pressure Regulator,“ International Journal of Pressure Vessels and Piping Article in Press, Corrected Proof available from www.sciencedirect.com.
7. Glière A. and Delattre C., "Modeling and fabrication of capillary stop valves for planar micro fluidic systems," Sensors and Actuators A: Physical, Volumes 130-131, 14 August 2006, pp. 601-608.
8. Eyabi, P. and Washington, G., "Modeling and sensorless control of an electromagnetic valve actuator," Mechatronics, Volume 16, Issues 3-4, April-May 2006, pp. 159-175.
9. Gölcü M., Sekmen, Y., Erduranlı, P., and Salman, M. S., "Artificial neural-network based modeling of variable valve-timing in a spark-ignition engine," Applied Energy, Volume 81, Issue 2, June 2005, pp.187-197.
10. Ning S. and Bone G.M., “development of a nonlinear dynamic model for a servo pneumatic positioning system,” 2005 Proceedings on IEEE Conference on Mechatronics and Automation, Niagara Falls, Canada.
11. Shoukat Choudhury M. A. A., Thornhill N. F. and Shah S. L., " Modeling valve stiction," Control Engineering Practice, Volume 13, Issue 5, May 2005, pp. 641-658.
12. M. A. A. Shoukat Choudhury, N. F. Thornhill and S. L. Shah Khoshzaban Zavarehi M; Lawrenece P. D.; Sassani F., “Nonlinear modeling and validation of solenoid-controlled pilot-operated servo valves,” IEEE/ASME Transactions on Mechatronics, Vol. 4, Issue 3, Sept. 1999, pp. 324-334.
13. Singhal A., Salsbury T.I., "A simple method for detecting valve stiction in oscillating control loops", Journal of process control, Vol. 15(2005), pp. 371-382.
14. Yamashita Y., "An automatic method for detection of valve stiction in process control loops", Control Engineering Practice, Vol. 14, (2006), pp. 503-510.

15. Tore Hagglund, "A friction compensator for pneumatic control valves", Journal of process control, Vol. 12(2002), pp. 897-904.
16. Stribeck, R. Die wesentlichen Eigenschaften der Gleit- und Rollenlager – The key qualities of sliding and roller bearings. Zeitschrift des Vereines Seutscher Ingenieure, 46H38, 39I: 1342–48, 1432–37, 1902.
17. C. Canudas de Wit, H. Olsson, K. J. Åström, and P. Lischinsky. A new model for control of systems with friction. 40(3), 1995.
18. Bliman, P. A., and Sorine, M. Friction modeling by hysteresis operators. application to Dahl, stiction and Stribeck effects. In Proceedings of the Conference "Models of Hysteresis", Trento, Italy, 1991.
19. Bliman, P. A., and Sorine, M. A system-theoretic approach of systems with hysteresis. Application to friction modeling and compensation. Proceedings of the second European Control Conference, Groningen, The Netherlands, pages 1844–49, 1993.
20. Bliman, P. A. and Sorine, M. Easy-to-use realistic dry friction models for automatic control. Proceedings of 3rd European Control Conference, Rome, Italy, pages 3788–3794, 1995.
21. Olsson, H. Control Systems with Friction. PhD thesis, Lund Institute of Technology, University of Lund, 1996.
22. Karimi, H., Nassirharand, A., and Beheshti, M., "Dynamic and nonlinear simulation of liquid propellant engines," AIAA Journal of Propulsion and Power, Vol. 19, (2003), pp. 938-944.
23. Idelchik, I.E., Jaico Publishing House, Handbook of Hydraulic Resistance, 3rd Edition.
24. Shoukat Choudhury, M.A.A., Shah, S.L., Thornhill, N.F., S. Shook, D., "Detection and Quntification of Control Valve Stiction," Control Science Direction, Engineering Practice, Vol. 14 (2006) pp. 1395–1412.
25. Chalupa, P., Novak, J., Bobal, V., "Modeling of Hydraulic Control Valves," *Recent Researches in Automatic Control,* (2011), pp.195-200
26. Sheng Nian, C., Hai Yang, L., Cheng Tao, X., and Bao Lin, P., "Proportional Solenoid Valve Flow Hysteresis Modeling Based on PSO Algorithm," Third International Conference on Instrumentation, Measurement, Computer, Communication and Control, 2013.